Inorganic Chemistry

Article

pubs.acs.org/IC

Proton-Coupled Electron Transfer between 4-Cyanophenol and Photoexcited Rhenium(I) Complexes with Different Protonatable Sites

Catherine Bronner and Oliver S. Wenger*

Georg-August-Universität, Institut für Anorganische Chemie, Tammannstrasse 4, D-37077 Göttingen, Germany

Supporting Information

ABSTRACT: Two rhenium(I) tricarbonyl diimine complexes, one of them with a 2,2′-bipyrazine (bpz) and a pyridine (py) ligand in addition to the carbonyls ([Re(bpz)-$(CO)_3$(py)]$^+$), and one tricarbonyl complex with a 2,2′-bipyridine (bpy) and a 1,4-pyrazine (pz) ligand ([Re(bpy)-$(CO)_3$(pz)]$^+$) were synthesized, and their photochemistry with 4-cyanophenol in acetonitrile solution was explored. Metal-to-ligand charge transfer (MLCT) excitation occurs toward the protonatable bpz ligand in the [Re(bpz)-$(CO)_3$(py)]$^+$ complex while in the [Re(bpy)$(CO)_3$(pz)]$^+$ complex the same type of excitation promotes an electron away from the protonatable pz ligand. This study aimed to explore how this difference in electronic excited-state structure affects the rates and the reaction mechanism for photoinduced proton-coupled electron transfer (PCET) between 4-cyanophenol and the two rhenium(I) complexes. Transient absorption spectroscopy provides clear evidence for PCET reaction products, and significant H/D kinetic isotope effects are observed in some of the luminescence quenching experiments. Concerted proton−electron transfer is likely to play an important role in both cases, but a reaction sequence of proton transfer and electron transfer steps cannot be fully excluded for the 4-cyanophenol/[Re(bpz)$(CO)_3$(py)]$^+$ reaction couple. Interestingly, the rate constants for bimolecular excited-state quenching are on the same order of magnitude for both rhenium(I) complexes.

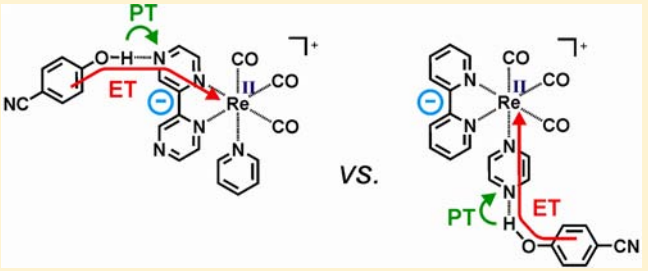

INTRODUCTION

In view of the importance of proton-coupled electron transfer (PCET) in photosynthesis,[1−3] respiration,[4] and nitrogen or carbon dioxide fixation,[5] there have been numerous investigations exploring the fundamentals of PCET in recent years.[6−10] Phenols have played a prominent role in such studies,[11−16] partly because phenolic functions occur in biologically relevant PCET systems, but also because they are simple enough for mechanistic investigations in purely artificial systems. A question of central interest in such studies is often whether the electron and the proton are transferred in a concerted manner or whether there are individual (consecutive) steps of electron transfer and proton transfer.[17,18] A variety of different experimental techniques have been employed including electrochemical,[10,15] EPR,[19] and optical spectroscopic methods.[20,21]

Many experimental investigations performed until now focus on PCET between molecules in their electronic ground states, but recently there has been increasing interest in PCET reactivity of photoexcited molecules or metal complexes.[22−33] Such investigations appear interesting in the context of direct light-to-chemical energy conversion, but much is yet to be learned about PCET involving electronically excited states.[28]

Against this background we have conducted a comparative study of the excited-state PCET chemistry of the two rhenium(I) tricarbonyl diimine complexes shown in Scheme 1 with 4-cyanophenol as a common reaction partner. Rhenium complexes of this type have long been known as luminophors and photooxidants,[34−37] and they were frequently employed as sensitizers for photoinduced electron transfer.[38−44] Both complexes from Scheme 1 have protonatable nitrogen atoms at the ligand periphery, either at a 2,2′-bipyrazine (bpz) chelating agent (left) or at a monodentate 1,4-pyrazine (pz) ligand (right). On the basis of prior studies of photoexcited ruthenium(II) 2,2′-bipyrazine complexes with phenols as reaction partners we anticipated that photoexcitation of the two rhenium complexes from Scheme 1 would induce PCET chemistry when 4-cyanophenol is present at sufficiently high concentration.[25,28,29,33] On the basis of these prior investigations we pictured that in aprotic solvent 4-cyanophenol might form hydrogen bonds to the bpz ligand of [Re(bpz)-$(CO)_3$(py)]$^+$ (py = pyridine) and to the pz ligand of [Re(bpy)$(CO)_3$(pz)]$^+$ (bpy = 2,2′-bipyridine), and such encounter adducts would appear to be reasonable precursors for PCET events.

The long-lived ^{3}MLCT (metal-to-ligand charge transfer) state which is populated after photoexcitation is localized on the bidentate bpz and bpy ligands (upper half of Scheme 1). Consequently, MLCT excitation of [Re(bpz)$(CO)_3$(py)]$^+$ is

Received: April 23, 2012
Published: July 17, 2012

   dx.doi.org/10.1021/ic300834c | Inorg. Chem. 2012, 51, 8275−8283

Scheme 1. MLCT Excitation and PCET Chemistry in Two Distinct 4-Cyanophenol/Rhenium Reaction Couples[a]

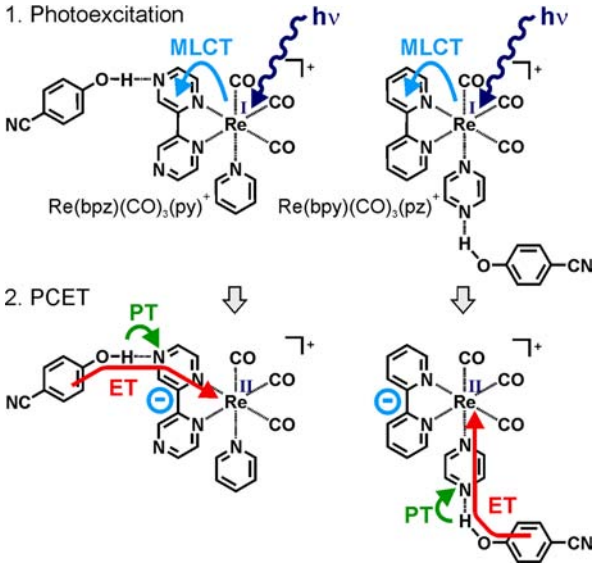

[a]ET = electron transfer, PT = proton transfer.

expected to increase the basicity of the nitrogen atoms at the periphery of the bpz ligand relative to the ground state (which is beneficial for proton transfer), but at the same time the MLCT-excited electron is in the middle of the electron transfer pathway between 4-cyanophenol and the metal center (lower left corner of Scheme 1). By contrast, MLCT excitation of $[Re(bpy)(CO)_3(pz)]^+$ opens a direct electron transfer pathway from the phenol to the metal center (lower right corner of Scheme 1), but MLCT excitation in this case is expected to decrease the basicity of the uncoordinated pz nitrogen atom relative to the ground state. We deemed it interesting to explore to what extent, if at all, these two fundamentally different scenarios affect the photoinduced chemistry of 4-cyanophenol/rhenium reaction couples.

RESULTS AND DISCUSSION

X-ray Crystal Structures. Yellow monocrystals of $[Re(bpz)(CO)_3(py)](PF_6)$ were grown by slow diffusion of pentane into an acetone solution. This compound crystallizes in the monoclinic $C2/c$ space group with two molecules of the complex and two hexafluorophosphate counterions in the asymmetric unit. The $[Re(bpz)(CO)_3(py)]^+$ cation is depicted in Figure 1a (note that only one crystallographically independent cation is represented). A solvate of this structure has already been described by Rillema et al.[45]

The $[Re(bpy)(CO)_3(pz)]^+$ complex (Figure 1b) was crystallized as the hexafluorophosphate salt by slow evaporation of acetone in an acetone/water mixture at 0 °C, affording yellow plates of $[Re(bpy)(CO)_3(pz)]_2(PF_6)_2\cdot(H_2O)\cdot((CH_3)_2CO)$. The complex crystallizes in the monoclinic $C2/c$ space group with one rhenium(I) complex and one PF_6^- ion in the asymmetric unit. In addition, a disordered acetone solvent molecule and a water molecule are present, the latter being located on a C_2 axis.

In both structures, the rhenium center has its three carbonyl ligands arranged to form the fac-isomer, as is commonly the case for this class of complexes. The coordination sphere is completed by a chelating bpz or bpy ligand and a monodentate

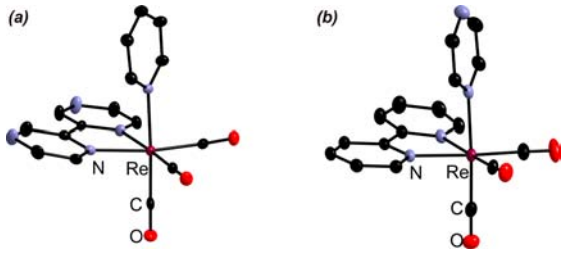

Figure 1. Crystal structures of the $[Re(bpz)(CO)_3(py)]^+$ (a) and $[Re(bpy)(CO)_3(pz)]^+$ (b) cations as found in $[Re(bpz)(CO)_3(py)](PF_6)$ and $[Re(bpy)(CO)_3(pz)]_2(PF_6)_2\cdot(H_2O)\cdot((CH_3)_2CO)$, respectively. Thermal ellipsoids are depicted at the 50% probability level. Hydrogen atoms are omitted for clarity.

py or pz ligand to form an octahedral coordination polyhedron with ligand−metal−ligand angles ranging from 74.84° to 99.18°. The Re−N bond distances are shorter for the chelating bpz and bpy agents than for the monodentate py and pz ligands (Table 1), indicating that the bidentate ligands are bound more

Table 1. Selected Average Bond Distances[a]

	Re−N_{bpy}	Re−N_{bpz}	Re−N_{py}	Re−N_{pz}	Re−C
$[Re(bpz)(CO)_3(py)]^+$		2.167	2.204		1.924
$[Re(bpy)(CO)_3(pz)]^+$	2.169			2.209	1.924

[a]In units of Å.

strongly to the metal than the monodentate ligands, as is expected.[46] All Re−C bonds are almost of equal length, showing no elongation in any position (an averaged distance is given in Table 1).

$[Re(bpy)(CO)_3(pz)]^+$ Luminescence Quenching. The optical absorption, luminescence, and electrochemical properties of $[Re(bpz)(CO)_3(py)]^+$ and $[Re(bpy)(CO)_3(pz)]^+$ have been previously explored.[45,47−50] Both complexes are emissive from ^{3}MLCT states in CH_3CN at room temperature, albeit with significantly different lifetimes (τ): In aerated CH_3CN at 25 °C τ = 182 ns for $[Re(bpy)(CO)_3(pz)]^+$ while τ = 31 ns for $[Re(bpz)(CO)_3(py)]^+$. For the purpose of the present study it was useful to include $[Re(bpy)(CO)_3(py)]^+$ as a reference complex with similar electronic structure, but lacking any protonatable sites at the ligand peripheries. This reference complex exhibits a ^{3}MLCT lifetime of 658 ns under the conditions mentioned above.[34]

Figure 2 shows the results of luminescence quenching experiments performed with the $[Re(bpy)(CO)_3(pz)]^+$ complex and 4-cyanophenol (CN-PhOH). The solvent was dried acetonitrile[51] because 4-cyanophenol concentrations of up to ~1.2 M can easily be achieved in this aprotic solvent. The luminescence intensities (Figure 2a) and lifetimes (Figure 2b) are both found to decrease with increasing 4-cyanophenol concentration. The luminescence intensity at λ_{max} = 542 nm decreases by roughly a factor of 5 between solutions containing 0 M and ~1 M 4-cyanophenol, but with increasing 4-cyanophenol concentration one detects increasingly intense emission bands in the spectral range between 400 and 500 nm. These latter bands are also observed from acetonitrile solutions containing only 4-cyanophenol (Figure S1 of the Supporting Information; these bands actually have a tail up to ~650 nm), and therefore are attributed to emission either from 4-cyanophenol or an emissive impurity with which our 4-

dx.doi.org/10.1021/ic300834c | Inorg. Chem. 2012, 51, 8275−8283

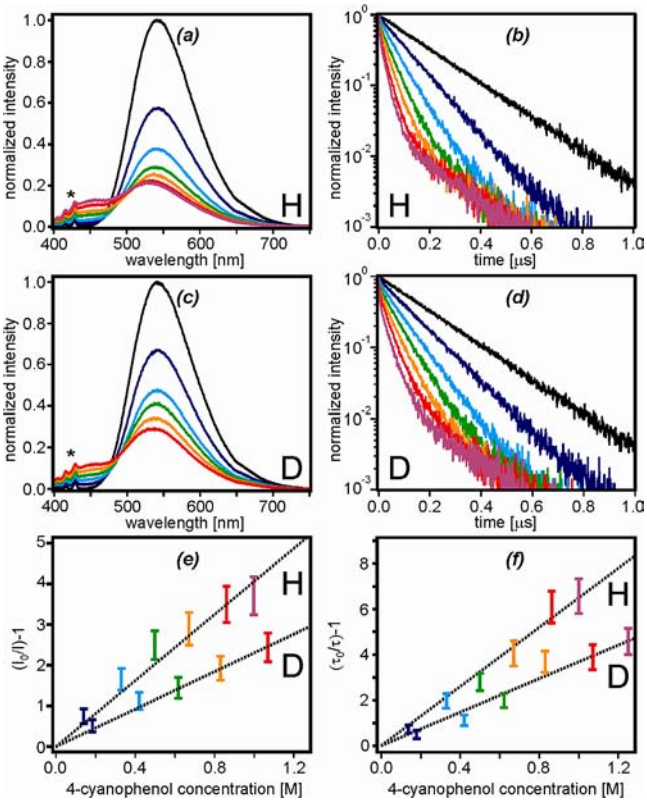

Figure 2. (a, c) Luminescence of $[Re(bpy)(CO)_3(pz)]^+$ in CH_3CN in presence of variable amounts of CN-PhOH (a) and CN-PhOD (c) after excitation at 380 nm. (b, d) Luminescence decays of the same complex detected at 542 nm under identical conditions following pulsed excitation at 340 nm. (e, f) Stern–Volmer plots based on the luminescence intensity (e) and lifetime (f) data. A consistent color code was used for all data; the concentrations used for the absorption and emission data in parts a–d can be read out from the Stern–Volmer plots in parts e and f. The *y*-axes in parts a–d are in arbitrary units. The asterisks in parts a and c denote Raman scattering peaks.

cyanophenol source is contaminated. The latter assignment makes particular sense because 4-cyanophenol does essentially not absorb at 380 nm, not even at 1 M concentration ($\varepsilon_{380\ nm} \approx 0.03\ M^{-1}\ cm^{-1}$; Figure S2). No correction for the impurity emission intensity at 542 nm was applied in the case of the $[Re(bpy)(CO)_3(pz)]^+$ data because the impurity emission is much weaker than that of the rhenium complex.

The $[Re(bpy)(CO)_3(pz)]^+$ luminescence lifetime decreases from 182 ns in the absence of 4-cyanophenol to 24 ns in presence of ~1 M phenolic quencher (Figure 2b). The decay curves remain single exponential up to 4-cyanophenol concentrations of 0.33 M and then become biexponential with a slower decay component exhibiting a lifetime of ~200 ns. This observation may be a manifestation of static quenching in phenol–rhenium adducts that are preassociated before photoexcitation, but we note that even at the highest phenol concentration the slow decay component contributes only 5% to the total emission decay. Consequently, the data analysis below will be based on the assumption of dynamic emission quenching, as is customary when emission lifetimes and intensities are both dependent on the quencher concentration.[52]

Analogous luminescence quenching experiments were performed with deuterated 4-cyanophenol (CN-PhOD), and the results are shown in Figure 2c,d. Even though the CN-PhOD concentrations in Figure 2c,d were somewhat higher than those of CN-PhOH represented with equal colors in Figure 2a,b, careful inspection of the data reveals that quenching is less pronounced when the phenol is in its deuterated form.

The magnitude of the H/D kinetic isotope effect (KIE) for ^{3}MLCT excited-state quenching of $[Re(bpy)(CO)_3(pz)]^+$ by 4-cyanophenol can be estimated from the Stern–Volmer plots in Figure 2e,f. The error bars associated with the individual data points arise essentially from the experimental uncertainty in determining relative emission intensities and luminescence lifetimes, which, from experience, is assumed to be 10%. From a linear regression fit to the emission intensity data (Figure 2e) a Stern–Volmer quenching constant ($K_{SV,\ H}$) of 4.2 ± 0.2 M^{-1} is obtained for CN-PhOH (R^2 = 0.9856) while $K_{SV,D}$ = 2.3 ± 0.1 M^{-1} for CN-PhOD (R^2 = 0.9980).[53] Given an inherent ^{3}MLCT lifetime (τ_0) of 182 ns for the $[Re(bpy)(CO)_3(pz)]^+$ complex in aerated CH_3CN, one finds bimolecular quenching constants of $k_{Q,H} = (2.3 \pm 0.1) \times 10^7\ M^{-1}\ s^{-1}$ and $k_{Q,D} = (1.3 \pm 0.1) \times 10^7\ M^{-1}\ s^{-1}$ for undeuterated and deuterated 4-cyanophenol, respectively (Table 2). The ratio between $k_{Q,H}$ and $k_{Q,D}$ yields an H/D KIE of 1.8 ± 0.2, suggesting that the rate-determining excited-state deactivation step involves proton motion.

Stern–Volmer analysis of the emission lifetimes (Figure 2f) leads us to the same conclusion. The Stern–Volmer constants in this case are $K_{SV,\ H}$ = 6.5 ± 0.2 M^{-1} (R^2 = 0.9941) and $K_{SV,\ D}$ = 3.7 ± 0.2 M^{-1} (R^2 = 0.9838), the bimolecular quenching constants are $k_{Q,\ H} = (3.6 \pm 0.1) \times 10^7\ M^{-1}\ s^{-1}$ and $k_{Q,\ D} = (2.0 \pm 0.1) \times 10^7\ M^{-1}\ s^{-1}$ (Table 2). Thus, an H/D KIE of 1.8 ± 0.2 is found from the lifetime data, in agreement with the value extracted from the emission intensities.

$[Re(bpz)(CO)_3(py)]^+$ Luminescence Quenching. Analogous emission quenching experiments as reported in the prior section were performed with the $[Re(bpz)(CO)_3(py)]^+$ complex; the excitation wavelength (λ_{exc}) in this case was 400 nm. The results are shown in Figure 3. An important difference to the $[Re(bpy)(CO)_3(pz)]^+$ complex is the comparatively short ^{3}MLCT lifetime of $[Re(bpz)(CO)_3(py)]^+$ (τ_0 = 31 ns in CH_3CN at 25 °C), presumably the consequence of more efficient multiphonon relaxation from the ^{3}MLCT state which is lower in energy in the bpz complex than in the bpy

Table 2. Stern–Volmer Constants (K_{SV}), Rate Constants for Bimolecular Excited-State Quenching (k_Q), and H/D Kinetic Isotope Effects (KIE) for the Two Reaction Couples As Determined from Emission Intensities and Lifetimes of the $[Re(bpy)(CO)_3(pz)]^+$ (bpy/pz) or $[Re(bpz)(CO)_3(py)]^+$ (bpz/py) Complexes

complex	exp type	$K_{SV,\ H}$ [M^{-1}]	$K_{SV,\ D}$ [M^{-1}]	$k_{Q,\ H}$ [$M^{-1}\ s^{-1}$]	$k_{Q,\ D}$ [$M^{-1}\ s^{-1}$]	KIE
bpy/pz	intensity	4.2 ± 0.2	2.3 ± 0.1	$(2.3 \pm 0.1) \times 10^7$	$(1.3 \pm 0.1) \times 10^7$	1.8 ± 0.2
bpy/pz	lifetime	6.5 ± 0.2	3.7 ± 0.2	$(3.6 \pm 0.1) \times 10^7$	$(2.0 \pm 0.1) \times 10^7$	1.8 ± 0.2
bpz/py	intensity	1.02 ± 0.02	0.87 ± 0.03	$(3.3 \pm 0.1) \times 10^7$	$(2.8 \pm 0.1) \times 10^7$	1.2 ± 0.1
bpz/py	lifetime	0.63 ± 0.03	0.43 ± 0.03	$(2.0 \pm 0.1) \times 10^7$	$(1.4 \pm 0.1) \times 10^7$	1.4 ± 0.2

dx.doi.org/10.1021/ic300834c | Inorg. Chem. 2012, 51, 8275–8283

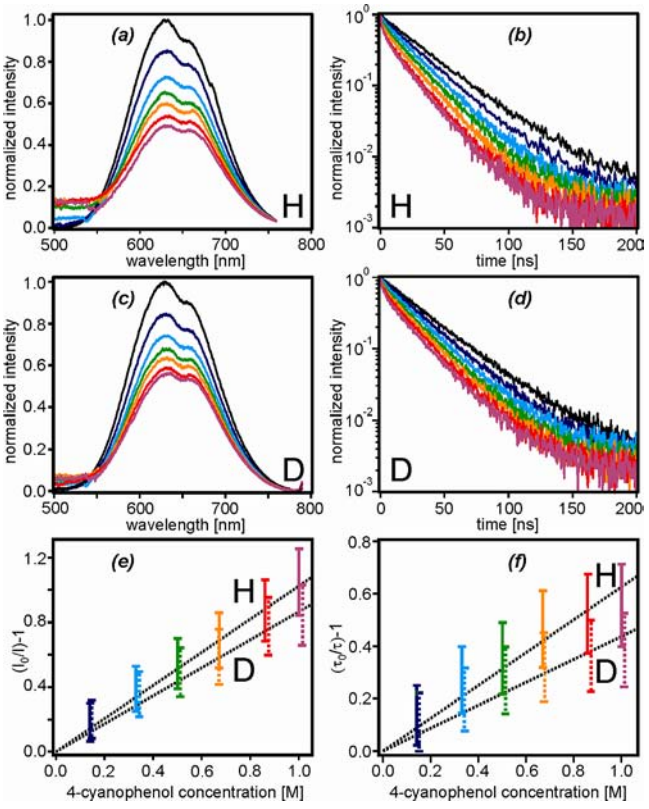

Figure 3. (a, c) Luminescence of $[Re(bpz)(CO)_3(py)]^+$ in CH_3CN in presence of variable amounts of CN-PhOH (a) and CN-PhOD (c) after excitation at 400 nm. (b, d) Luminescence decays of the same complex detected at 630 nm under identical conditions following pulsed excitation at 340 nm. (e, f) Stern–Volmer plots based on the luminescence intensity (e) and lifetime (f) data. A consistent color code was used for all data; the concentrations used for the absorption and emission data in parts a–d can be read out from the Stern–Volmer plots in parts e and f. The *y*-axes in parts a–d are in arbitrary units.

complex.[54] The decrease in ^{3}MLCT energy also manifests in a red-shift of the emission band maximum ($\lambda_{max} \approx 644$ nm)[55] relative to that of $[Re(bpy)(CO)_3(pz)]^+$ ($\lambda_{max} = 542$ nm), and a weaker luminescence quantum yield. The statement regarding quantum yields is made on the basis of the observation of rhenium emission (between 550 and 750 nm) and impurity emissions (between 400 and 650 nm, see above) which are on the same order of magnitude (Figure S3). In the spectra shown in Figure 3a,c the impurity emission has been subtracted (see the Supporting Information for details).

The luminescence decays detected at 630 nm also exhibit signs of impurity emission when 4-cyanophenol is added to a solution of $[Re(bpz)(CO)_3(py)]^+$. Specifically, the decays are found to be triexponential even at moderate quencher concentrations. Measurements on CH_3CN solutions containing 4-cyanophenol but no rhenium show that two of the three decay components at 630 nm ($\tau_1 \approx 1.1$ ns and $\tau_2 \approx 4.5$ ns) are due to the emissive impurity (Figure S4). Consequently, only the slowest decay component ($\tau_3 > 10$ ns) is of interest in the luminescence quenching experiments from Figure 3b,d.

Stern–Volmer analysis of the intensity and lifetime data in Figure 3a–d results in the plots in Figure 3e,f, and linear regression fits (R^2 values range from 0.9743 to 0.9985) yield Stern–Volmer constants ($K_{SV,H}$, $K_{SV,D}$) and bimolecular excited-state quenching constants ($k_{Q,H}$, $k_{Q,D}$) as reported in Table 2.[56] The $k_{Q,H}$ and $k_{Q,D}$ values for $[Re(bpz)(CO)_3(py)]^+$ turn out to be on the same order of magnitude as for $[Re(bpy)(CO)_3(pz)]^+$ (between $(1.4 \pm 0.1) \times 10^7$ M^{-1} s^{-1} and $(3.3 \pm 0.1) \times 10^7$ M^{-1} s^{-1}); the luminescence quenching observed in Figure 3a–d is less pronounced than in Figure 2a–d simply because $[Re(bpz)(CO)_3(py)]^+$ has a lower emission quantum yield and a shorter excited-state lifetime than $[Re(bpy)(CO)_3(pz)]^+$. On the basis of the $k_{Q,H}$ and $k_{Q,D}$ values for $[Re(bpz)(CO)_3(py)]^+$ we obtain KIE = 1.2 ± 0.1 (from emission intensities) and 1.4 ± 0.2 (from lifetimes).

Transient Absorption Spectroscopy. In order to identify the photoproducts of the reaction between 4-cyanophenol and the photoexcited rhenium complexes transient absorption spectroscopy is a useful technique. Figure 4 shows the results

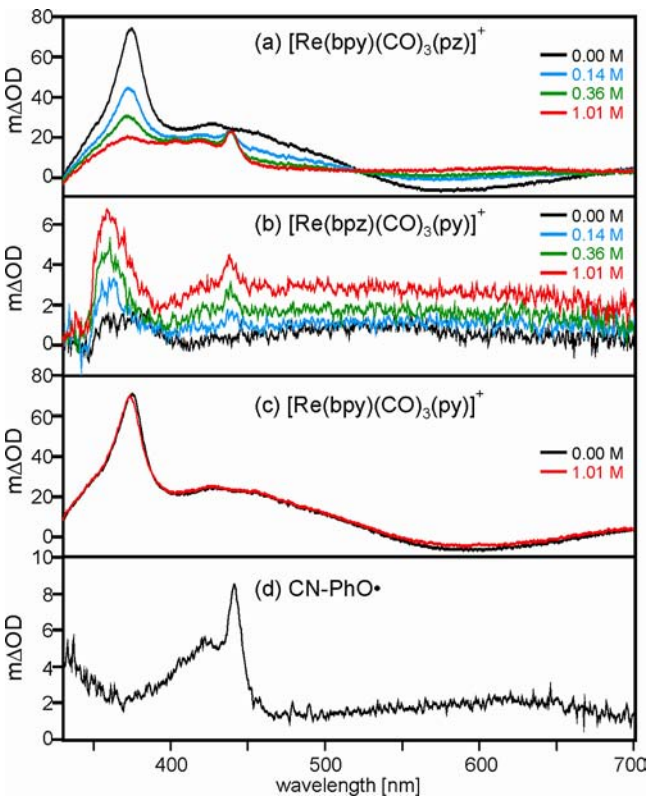

Figure 4. (a) Transient absorption spectra obtained from $\sim 10^{-5}$ M $[Re(bpy)(CO)_3(pz)]^+$ solutions in CH_3CN in presence of variable concentrations of CN-PhOH (see inset). The data is time-averaged over 200 ns after excitation at 355 nm with ~8 ns pulses. An identical set of data is shown for the $[Re(bpz)(CO)_3(py)]^+$ complex in part b and for the $[Re(bpy)(CO)_3(py)]^+$ reference complex in part c. (d) Transient absorption spectrum obtained from a $\sim 10^{-5}$ M solution of 4-cyanophenol in a 1:1 (v:v) mixture of CH_3CN and di-*tert*-butyl peroxide after excitation at 355 nm with ~8 ns pulses.

from such experiments in which $\sim 10^{-5}$ M solutions of $[Re(bpy)(CO)_3(pz)]^+$ (a), $[Re(bpz)(CO)_3(py)]^+$ (b),[57] and $[Re(bpy)(CO)_3(py)]^+$ (c) containing between 0 and ~1 M 4-cyanophenol were irradiated at 355 nm with laser pulses of ~8 ns duration; the spectra are time-averaged over the first 200 ns after excitation. In the absence of quencher (black traces) an intense and relatively narrow absorption band is observed for $[Re(bpy)(CO)_3(pz)]^+$ (a) and $[Re(bpy)(CO)_3(py)]^+$ (c) at 375 nm, while in $[Re(bpz)(CO)_3(py)]^+$ (b) there is a weaker band at 370 nm. On the basis of prior transient absorption studies of chemically closely related rhenium(I) tricarbonyl

dx.doi.org/10.1021/ic300834c | *Inorg. Chem.* 2012, 51, 8275–8283

Scheme 2. Possible PCET Reaction Pathways

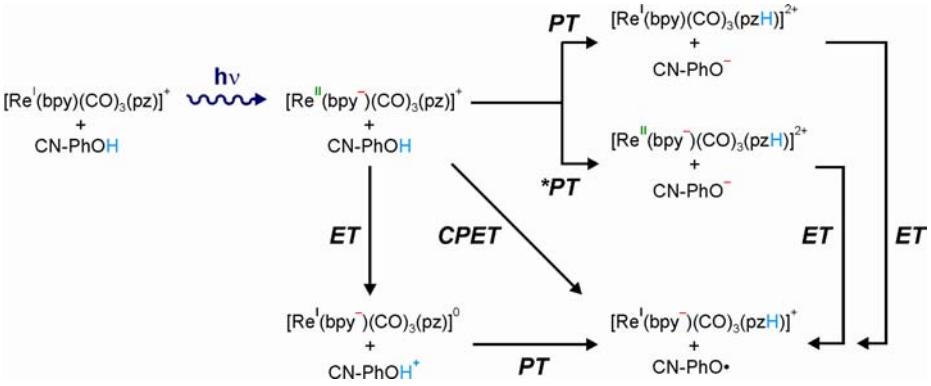

diimines, the respective bands are assigned to the reduced α-diimine ligand (bpy or bpz) of the ^{3}MLCT-excited complexes.[38,48,58,59]

Upon addition of 4-cyanophenol significant spectral changes occur in the transient absorption spectra of Figure 4a,b, while the spectrum of the reference complex (Figure 4c) stays essentially unchanged even after adding ~1 M CN-PhOH. The latter observation shows that 4-cyanophenol is unable to quench the ^{3}MLCT excited-state of $[Re(bpy)(CO)_3(py)]^+$, and this is corroborated by luminescence experiments (Figure S8 of the Supporting Information).

In the cases of the two complexes with protonatable ligands there is a relatively narrow absorption band at 440 nm which gains intensity with increasing 4-cyanophenol concentration. A prior study reported that the 4-cyanophenoxyl radical (CN-PhO$^\bullet$) exhibits an absorption maximum at 443 nm.[60] In order to test whether the 440-nm band observed in Figure 4a,b could indeed be due to CN-PhO$^\bullet$, we dissolved 4-cyanophenol in a 1:1 (v:v) mixture of acetonitrile and di-*tert*-butyl peroxide,[61] and recorded the optical absorption spectrum after exciting the sample at 355 nm with laser pulses of ~8 ns duration. The result of this experiment is shown in Figure 4d and demonstrates quite convincingly that the 440 nm absorption (and the weaker sideband at 420 nm) is due to CN-PhO$^\bullet$; in fact the spectrum in Figure 4d is quite typical for phenoxyl radicals.[60−63]

The direct observation of 4-cyanophenoxyl radical in transient absorption strongly suggests that PCET chemistry occurs between 4-cyanophenol and the photoexcited $[Re(bpy)(CO)_3(pz)]^+$ and $[Re(bpz)(CO)_3(py)]^+$ complexes, even though we cannot unambiguously identify protonated and reduced rhenium products. Whether the CN-PhO$^\bullet$ species is formed through concerted proton−electron transfer (CPET) or consecutive electron transfer (ET) and proton transfer (PT) steps (in whatever sequence) cannot be determined from our transient absorption experiments, mainly because the temporal resolution is too low.

The photoproduction of phenoxyl radicals implies the simultaneous formation of a rhenium reduction product, either a $[Re^I(bpy^-)(CO)_3(pz)]$ (Figure 4a) or a $[Re^I(bpz^-)(CO)_3(py)]$ species (Figure 4b).[81] The respective species formally contain reduced bpy and bpz ligands, analogously to the ^{3}MLCT-excited forms of these complexes. Rhenium tricarbonyl diimines therefore usually exhibit similar transient absorption spectra in their one-electron reduced forms and in their ^{3}MLCT-excited forms,[82] with the signal observed at ~375 nm in Figure 4a−c being the strongest absorption of bpy$^-$ or bpz$^-$. It appears that the one-electron reduced form of $[Re(bpy)(CO)_3(pz)]^+$ (red trace in Figure 4a) has a weaker extinction coefficient at 375 nm than the ^{3}MLCT-excited form of this complex (black trace in Figure 4a), but the reasons for this observation are unclear. What seems clear, however, is that the 375-nm band is also present in the spectrum of the $[Re^I(bpy^-)(CO)_3(pz)]$ species (red trace in Figure 4a); the phenoxyl radical absorption has a *minimum* at ~375 nm (Figure 4d) while there is clearly a local *maximum* near 375 nm in the red spectrum of Figure 4a. Thus, there is direct evidence not only for a phenol oxidation product but also for a rhenium reduction product in all relevant cases.

Given the experimental uncertainty associated with the luminescence quenching experiments performed with $[Re(bpz)(CO)_3(py)]^+$ (Figure 3), transient absorption studies would in principle be helpful to obtain complementary information about the reaction kinetics, but the temporal resolution of our transient absorption setup is insufficient for this purpose.

Driving-Force and Mechanistic Considerations. Scheme 2 illustrates possible PCET reaction pathways for the 4-cyanophenol/$[Re(bpy)(CO)_3(pz)]^+$ reaction couple. Aside from simple (radiative or nonradiative) relaxation to the ground state, four different deactivation processes are conceivable once the metal complex has been photoexcited: (i) photoinduced electron transfer followed by proton transfer (i. e., reaction along the lower left corner; ET, PT); (ii) photoinduced proton transfer to produce an excited deprotonated complex followed by electron transfer (*PT, ET); (iii) photoinduced proton transfer to produce deprotonated complex in its electronic ground state followed by electron transfer (PT, ET); (iv) concerted proton−electron transfer (CPET). Some thermodynamic considerations appear useful for elucidating which reaction pathways may be viable in our systems.[6,17,64]

The electrochemical properties of the $[Re(bpz)(CO)_3(py)]^+$, $[Re(bpy)(CO)_3(pz)]^+$, and $[Re(bpy)(CO)_3(py)]^+$ complexes in acetonitrile have been previously investigated.[34,45,47,50,65] Electrochemical potentials for one-electron reduction were generally reported versus the saturated calomel electrode, and in Table 3 we have converted the respective values to potentials (E_{red}) versus the ferrocenium/ferrocene (Fc^+/Fc) couple (by subtracting 0.38 V from the previously published values).[66] The reduction potentials of the ^{3}MLCT-excited complexes were estimated by adding the energy of the MLCT state (E_{MLCT}) to the ground-state reduction potentials, as is common practice.[67,68] From the last column in Table 3 we learn that the reduction potentials of the ^{3}MLCT-excited complexes are

dx.doi.org/10.1021/ic300834c | *Inorg. Chem.* 2012, 51, 8275−8283

Table 3. Electrochemical Potentials for One-Electron Reduction of the $[Re(bpy)(CO)_3(pz)]^+$ (bpy/pz), $[Re(bpz)(CO)_3(py)]^+$ (bpz/py), and $[Re(bpy)(CO)_3(py)]^+$ (bpy/py) Complexes in the Electronic Ground State (E_{red}) and in the ^{3}MLCT Excited State (E^*_{red}) in Volts vs Fc^+/Fc with E_{MLCT} the Energy of the ^{3}MLCT State

complex	E_{red} [V]	E_{MLCT} [eV]	E^*_{red} [V]
bpy/pz	−1.59[b]	2.26[f]	0.67
bpz/py	−1.03[c]	2.05[g]	1.02
bpy/py	−1.49[d]	2.26[h]	0.77
bpy/pz-CH_3[a]	−0.55[e]	2.26[f]	1.71

[a]pz-CH_3 denotes a 1,4-pyrazine ligand which has been methylated at the peripheral N-atom. [b]From ref 50. [c]From ref 48. [d]From ref 34. [e]From ref 65. [f]Estimated on the basis of E_{MLCT} in the bpy/pz complex and the reduction of the HOMO−LUMO energy gap between $[Re(bpy)(CO)_3(pz)]^+$ and $[Re(bpz)(CO)_3(py)]^+$.[45] [g]From ref 47. [h]Assumed to be identical to the bpy/pz complex because ^{3}MLCT emission involves the same type of bpy ligand.

either around 1.0 V versus Fc^+/Fc or below; the only exception is the dicationic $[Re(bpy)(CO)_3(pz\text{-}CH_3)]^{2+}$ complex having a methylated 1,4-pyrazine ligand which we will discuss later.

The electrochemical potential for one-electron oxidation of 4-cyanophenol (E_{ox}) has also been reported previously.[6,69,70] In acetonitrile solution, E_{ox} = 1.40 V versus Fc^+/Fc for CN-PhOH.[66,70] Consequently, initial photoinduced electron transfer to any of the three monocationic rhenium complexes of this study is thermodynamically improbable because this process is endergonic by ∼0.4 eV for $[Re(bpz)(CO)_3(py)]^+$, ∼0.6 eV for $[Re(bpy)(CO)_3(py)]^+$, and ∼0.7 eV for $[Re(bpy)(CO)_3(pz)]^+$. What is more, the comparatively large H/D KIE of 1.8 observed for $[Re(bpy)(CO)_3(pz)]^+$ (see above) cannot be reconciled with pure electron transfer in the rate-determining excited-state deactivation step.[8,9,18]

Thermodynamic data for the proton transfer steps of Scheme 2 is experimentally difficult to access. For ruthenium(II) complexes with protonatable bpz ligands acid−base titrations monitoring UV−vis spectral changes can yield information about the pK_a values in the different redox states of the metal center.[71−75] However, for our rhenium complexes the spectral changes occurring upon protonation are minor; there appears to be simply no good (optical spectroscopic) handle for determination of the ground-state pK_a values of $[Re(bpz)(CO)_3(py)]^+$ and $[Re(bpy)(CO)_3(pz)]^+$. However, it is possible to determine the pK_a values of the ^{3}MLCT-excited $[Re(bpz)(CO)_3(py)]^+$ and $[Re(bpy)(CO)_3(pz)]^+$ complexes using luminescence spectroscopy (Figure S5/S6 of the Supporting Information). The respective pK_a* values are 3.4 ± 0.5 for $[Re(bpy)(CO)_3(pz)]^+$ and 3.1 ± 0.5 for $[Re(bpy)(CO)_3(pz)]^+$ in 1:1 (v:v) CH_3CN/H_2O (Table S1 of the Supporting Information). 4-Cyanophenol has a pK_a value of 9.0 ± 0.2 under identical experimental conditions (Figure S7). Thus, protonation of the photoexcited metal complexes prior to electron transfer (*PT, ET sequence in Scheme 2) is thermodynamically unlikely.

However, we note that proton transfer coupled to electronic relaxation of the ^{3}MLCT-excited complexes to their ground states (PT step in Scheme 2) is more exergonic by ∼E_{MLCT} than proton transfer to form rhenium complexes in their excited states (*PT step in Scheme 2); hence, there may be significant driving-force for the initial step of the PT, ET sequence of Scheme 2. However, on the basis of the (ground-state) reduction potential of the methylated $[Re(bpy)(CO)_3(pz\text{-}CH_3)]^{2+}$ complex (−0.55 V vs Fc^+/Fc; Table 3), and an oxidation potential of 0.15 V vs Fc^+/Fc for 4-cyanophenolate (in DMSO),[6,69] we estimate a reaction free energy of +0.7 eV for the ET step following the initial PT step in the 4-cyanophenol/$[Re(bpy)(CO)_3(pz)]^+$ reaction couple.[76] The highly endergonic nature of the subsequent ET step should preclude the formation of PCET photoproducts as observed experimentally, at least in the case of the $[Re(bpy)(CO)_3(pz)]^+$ complex (Figure 4b). No electrochemical data for methylated or protonated $[Re(bpz)(CO)_3(py)]^+$ is available, but given the observation that $[Re(bpz)(CO)_3(py)]^+$ is easier to reduce than $[Re(bpy)(CO)_3(pz)]^+$ by about 0.6 V (Table 3), the PT, ET sequence appears thermodynamically more realistic in this case.

In short, from a thermodynamic perspective CPET appears as the most plausible PCET reaction mechanism of the 4-cyanophenol/rhenium couples; for the $[Re(bpz)(CO)_3(py)]^+$ complex the PT, ET sequence cannot be fully excluded.

SUMMARY AND CONCLUSIONS

The rhenium complexes used in this study are less practical chromophores than previously investigated $[Ru(bpy)_2(bpz)]^{2+}$ and $[Ru(bpz)_3]^{2+}$ complexes because protonation effects are difficult to detect by optical spectroscopic means. Nevertheless, transient absorption spectroscopy is able to provide clear evidence for PCET chemistry because the spectral fingerprint of the 4-cyanophenoxyl radical can be detected. From a thermodynamics perspective, CPET appears as the most plausible reaction mechanism for the 4-cyanophenol/$[Re(bpy)(CO)_3(pz)]^+$ couple, and the experimentally observed H/D KIE of 1.8 ± 0.2 is in line with this expectation. CPET is thermodynamically viable also in the case of $[Re(bpz)(CO)_3(py)]^+$, but a PT, ET sequence (involving electronic relaxation in the PT step) cannot be ruled out completely. A mixture of different mechanisms which are active at the same time cannot be excluded either; only an ET, PT contribution can be ruled out safely on the basis of thermodynamic grounds. Thus, mechanistically the case has not become as clear as we had originally hoped, but the interesting finding is that both rhenium complexes exhibit PCET chemistry with similar reaction rates even though they have different excited-state structures in the sense that different sites become protonatable after MLCT excitation. The bottom line is that for the reaction rates it does not appear to matter whether MLCT excitation occurs toward the protonatable ligand or away from it, at least for the two reaction couples investigated here.

EXPERIMENTAL SECTION

The rhenium(I) complexes were synthesized following previously published procedures;[34,77,83,84] column chromatography occurred on silica gel 60 from Machery-Nagel. Bruker Avance DRX 300 and B-ACS-120 instruments were used for ^{1}H NMR spectroscopy, electron ionization mass spectrometry (EI-MS) was performed on a Finnigan MAT8200 instrument, and for elemental analysis a Vario EL III CHNS analyzer from Elementar was employed. Synthetic protocols and product characterization data are as follows.

For $[Re(bpy)(CO)_3(pz)](PF_6)$, a 500 mg (1.38 mmol) portion of pentacarbonylchlororhenium(I) was suspended in 80 mL of toluene along with 220 mg (1.41 mmol) of 2,2′-bipyridine and heated to 110 °C for 7 h. After cooling to room temperature the yellow $Re(bpy)(CO)_3Cl$ precipitate (590 mg, 93%) was isolated by suction filtration. $Re(bpy)(CO)_3Cl$ was reacted with $AgPF_6$ (139 mg, 0.55 mmol) in 50 mL of CH_3CN at reflux for 13 h. After cooling to room temperature, the solution was filtered and the filtrate evaporated to

dx.doi.org/10.1021/ic300834c | Inorg. Chem. 2012, 51, 8275−8283

Table 4. Single Crystal X-ray Diffraction Parameters for $[Re(bpy)(CO)_3(pz)]_2(PF_6)_2\cdot(H_2O)\cdot((CH_3)_2CO)$ and $[Re(bpz)(CO)_3(py)](PF_6)$

	$[Re(bpz)(CO)_3(py)](PF_6)$	$[Re(bpy)(CO)_3(pz)]_2(PF_6)_2\cdot(H_2O)\cdot((CH_3)_2CO)$
formula	$C_{16}H_{11}F_6N_5O_3PRe$	$C_{37}H_{24}F_{12}N_8O_8P_2Re_2$
MW (g/mol)	652.47	1379.05
T (K)	100(2)	100(2)
cryst syst	monoclinic	monoclinic
space group	$C2/c$	$C2/c$
a (Å)	43.0640(13)	23.463(4)
b (Å)	9.7300(3)	9.4086(16)
c (Å)	20.6150(6)	21.361(3)
β (deg)	114.571(2)	109.374(8)
V (Å^3)	7855.8(4)	4448.5(13)
Z	16	4
D (g·cm^{-3})	2.207	2.059
$\mu_{MoK\alpha}$ (mm^{-1})	6.356	5.620
F_{000}	4960.0	2648.0
GOF	1.052	1.109
R_1 ($I > 2\,\sigma(I)$)[a]	0.0351	0.0174
wR_2 (all reflections)[b]	0.0897	0.0402

[a] $R_1 = \Sigma||F_o| - |F_c||/\Sigma|F_o|$. [b] $wR_2 = [\Sigma w(F_o^2 - F_c^2)^2/\Sigma w(F_o^2)^2]^{1/2}$, $w = 1/[\sigma^2(F_o^2) + (aP)^2 + bP]$ and $P = (F_o^2 + 2F_c^2)/3$.

yield $[Re(bpy)(CO)_3(CH_3CN)](PF_6)$. The latter material was refluxed in 10 mL of a 3:10 (v:v) mixture of CH_2Cl_2 and CH_3OH along with 1,4-pyrazine (900 mg, 11.2 mmol) for 42 h. The hot solution was filtered, and the filtrate was evaporated to dryness. Purification of the raw product occurred by column chromatography on silica gel using as an eluent first acetone, then a 10:1 (v:v) mixture of acetone and H_2O, and finally a 100:10:1 (v:v:v) mixture of acetone, H_2O, and saturated aqueous KNO_3 solution. Acetone was evaporated from the chromatography fractions containing the desired complex, and precipitation of its hexafluorophosphate salt was induced by addition of saturated aqueous KPF_6 solution. This procedure resulted in pure $[Re(bpy)(pz)(CO)_3](PF_6)$ in 37% yield (41 mg). ^{1}H NMR (CD_3CN, 300 MHz, 25 °C): δ [ppm] = 7.82 (ddd, J = 7.6, 5.5, 1.5 Hz, 2H), 8.24 (dd, J = 3.0, 1.5 Hz, 2H), 8.30 (td, J = 7.9, 1.5 Hz, 2H), 8.42 (d, J = 8.1 Hz, 2H), 8.57 (dd, J = 3.0, 1.5 Hz, 2H), 9.22 (d, J = 5.5 Hz, 2H). ES-MS m/z = 507.0461 (calcd 507.0463 for $C_{17}H_{12}N_4O_3Re^+$). Anal. Calcd for $C_{17}H_{12}N_4O_3PF_6Re$: C 31.34, H 1.86, N 8.60. Found: C 31.22, H 2.02, N 8.95.

For the synthesis of $[Re(bpy)(CO)_3(py)](CF_3SO_3)$, $[Re(bpy)(CO)_3(CH_3CN)](CF_3SO_3)$ which was available from prior studies[43,78] in 26 mL of a 3:10 (v:v) mixture of $CHCl_3$ and CH_3OH was added pyridine (30 μL, 0.38 mmol), and the solution was refluxed under N_2 overnight. Subsequent column chromatography on silica gel using a 9:1 (v:v) mixture of CH_2Cl_2/CH_3OH afforded the pure product in 65% yield (148 mg). ^{1}H NMR ($CDCl_3$, 300 MHz, 25 °C): δ [ppm] = 7.45−7.35 (m, 2H), 7.74 (ddd, J = 7.6, 5.5, 1.3 Hz, 2H), 7.86 (tt, J = 7.6, 1.6 Hz, 1H), 8.22−8.14 (m, 2H), 8.37 (td, J = 8.0, 1.6 Hz, 2H), 8.89 (d, J = 8.2 Hz, 2H), 9.11 − 9.03 (m, 2H). ES-MS m/z = 506.0507 (calcd 506.0510 for $C_{18}H_{13}N_3O_3Re^+$). Anal. Calcd for $C_{19}H_{13}N_3O_6F_3ReS$: C 34.86, H 2.00, N 6.42. Found: C 34.88, H 1.96, N 6.40.

For the synthesis of $[Re(bpz)(CO)_3(py)](PF_6)$, $Re(CO)_5Cl$ (330 mg, 1.00 mmol) and bpz (193 mg, 1.22 mmol) were refluxed in dry toluene overnight. After cooling to room temperature, the resulting purple solid is filtered and washed with pentane to yield $Re(bpz)(CO)_3Cl$ in 68% yield (320 mg). The latter complex was refluxed overnight in 12 mL of CH_3CN along with 40 mg (0.17 mmol) of $AgPF_6$. After cooling to room temperature the reaction mixture was filtrated to remove AgCl, and the filtrate was evaporated to dryness. The resulting orange solid was used for the next step without further purification. Pyridine (20 μL, 0.25 mmol) was added to a suspension of $[Re(bpz)(CO)_3(CH_3CN)](PF_6)$ (117 mg, 0.20 mmol) in 26 mL of a 3:10 (v:v) mixture of $CHCl_3$ and CH_3OH, and the reaction mixture was refluxed under N_2 for 15 h before evaporating the solvent. Product purification occurred by column chromatography on silica gel using as an eluent first pure acetone, then a 10:1 (v:v) mixture of acetone and H_2O, and finally a 100:10:1 (v:v:v) mixture of acetone, H_2O, and saturated aqueous KNO_3. Acetone was evaporated from the chromatography fractions containing the desired complex, and precipitation of its hexafluorophosphate salt was induced by addition of saturated aqueous KPF_6 solution. This procedure resulted in 47 mg of pure product (36% yield). ^{1}H NMR (acetone-d_6, 300 MHz, 25 °C): δ [ppm] = 7.65−7.36 (m, 2H), 8.05 (tt, J = 7.7, 1.5 Hz, 1H), 8.67 (dt, J = 5.0, 1.5 Hz, 2H), 9.26 (d, J = 3.1 Hz, 2H), 9.62 (dd, J = 3.1, 1.3 Hz, 2H), 10.18 (d, J = 1.3 Hz, 2H). ES-MS m/z = 508.0412 (calcd 508.0415 for $C_{16}H_{11}N_5O_3Re^+$). Anal. Calcd for $C_{16}H_{11}N_5O_3F_6PRe\cdot0.6C_3H_6O$: C 31.11, H 2.14, N 10.19. Found: C 31.18, H 2.01, N 10.39.

For deuteration, 4-cyanophenol was dissolved in methanol-d_4 (99.80% D) and stirred for 1 h under N_2 at room temperature. The solvent was removed subsequently using a rotary evaporator, and the operation was repeated a second time. This procedure resulted in isotope purity on the order of 99%. Acetonitrile for spectroscopic investigations was freshly distilled from P_2O_5. UV−vis spectroscopy was performed on a Cary 300 instrument. Luminescence spectra and lifetimes were measured a Fluorolog-322 spectrometer equipped with a TCSPC option (Fluorohub FL-1061PC) and a TBC-07C detector from Hamamatsu. For the lifetime experiments excitation occurred at 340 nm using a NanoLed-340 unit. Transient absorption experiments were conducted on an LP920-KS spectrometer from Edingburgh Instruments with a detection system composed of an iCCD camera from Andor and an R928 photomultiplier. Excitation occurred with the frequency-tripled output from a Quantel Brilliant b laser. All spectroscopy measurements occurred in aerated solution; the absorbance of the rhenium complexes at the excitation wavelength was typically between 0.1 and 0.3. The pH measurements occurred using a standard pH meter.

Single crystals of $[Re(bpz)(CO)_3(py)]_2(PF_6)_2(H_2O)((CH_3)_2CO)$ and $[Re(bpy)(CO)_3(pz)](PF_6)$ were coated with Paratone N-oil and mounted on a fiber loop followed by data collection at 100 K. The crystallographic data was collected with a Bruker APEX II diffractometer, equipped with a graphite monochromator centered on the path of Mo Kα (λ = 0.710 73 Å) radiation. The SAINT program was used to integrate the data, which was thereafter corrected for absorption using SADABS.[79] The structure was solved by direct methods and refined by least-squares fits on F^2 in SHELX97.[80] All non-hydrogen atoms were refined anisotropically by full-matrix least-squares (SHELXL-97). Hydrogen atoms were placed using a riding

dx.doi.org/10.1021/ic300834c | Inorg. Chem. 2012, 51, 8275−8283

model. Their positions were constrained relative to their parent atom using the appropriate HFIX command in SHELXL-97. In $[Re(bpy)(CO)_3(pz)]_2(PF_6)_2\cdot(H_2O)\cdot((CH_3)_2CO)$, the lattice acetone molecule was found to be disordered on two equivalent positions. Hydrogen atoms on this disordered acetone molecule and on the lattice water molecule were not introduced. Table 4 contains the summary of the unit cell and structure refinement parameters. The CIF files can be found in the Supporting Information. The CCDC numbers of the two structures are 877478 and 877479.

■ ASSOCIATED CONTENT

Supporting Information

Absorption and emission data of a sample from the 4-cyanophenol substance used in this work. Luminescence raw data from $[Re(bpz)(CO)_3(py)]^+$ and details regarding determination of (excited-state) pK_a values. Crystallographic data (CIF files). This material is available free of charge via the Internet at http://pubs.acs.org.

■ AUTHOR INFORMATION

Corresponding Author

*E-mail: oliver.wenger@chemie.uni-goettingen.de.

Notes

The authors declare no competing financial interest.

■ ACKNOWLEDGMENTS

The authors thank Dr. Pierre Dechambenoit (Université de Bordeaux) for X-ray data collection. Funding from the Deutsche Forschungsgemeinschaft (DFG) through Grants WE4815/1-1 and INST186/872-1 is gratefully acknowledged. The MWK Niedersachsen is thanked for co-funding the transient absorption setup.

■ REFERENCES

(1) Mayer, J. M.; Rhile, I. J.; Larsen, F. B.; Mader, E. A.; Markle, T. F.; DiPasquale, A. G. *Photosynth. Res.* **2006**, *87*, 3.

(2) Meyer, T. J.; Huynh, M. H. V.; Thorp, H. H. *Angew. Chem., Int. Ed.* **2007**, *46*, 5284.

(3) Hammarström, L.; Styring, S. *Energy Environ. Sci.* **2011**, *4*, 2379.

(4) Ramirez, B. E.; Malmström, B. G.; Winkler, J. R.; Gray, H. B. *Proc. Natl. Acad. Sci. U.S.A.* **1995**, *92*, 11949.

(5) Concepcion, J. J.; Jurss, J. W.; Brennaman, M. K.; Hoertz, P. G.; Patrocinio, A. O. T.; Iha, N. Y. M.; Templeton, J. L.; Meyer, T. J. *Acc. Chem. Res.* **2009**, *42*, 1954.

(6) Warren, J. J.; Tronic, T. A.; Mayer, J. M. *Chem. Rev.* **2010**, *110*, 6961.

(7) Dempsey, J. L.; Winkler, J. R.; Gray, H. B. *Chem. Rev.* **2010**, *110*, 7024.

(8) Hammes-Schiffer, S. *Acc. Chem. Res.* **2009**, *42*, 1881.

(9) Hammes-Schiffer, S.; Stuchebrukhov, A. A. *Chem. Rev.* **2010**, *110*, 6939.

(10) Costentin, C.; Robert, M.; Savéant, J.-M. *Acc. Chem. Res.* **2010**, *43*, 1019.

(11) Biczok, L.; Gupta, N.; Linschitz, H. *J. Am. Chem. Soc.* **1997**, *119*, 12601.

(12) Fang, Y.; Liu, L.; Feng, Y.; Li, X. S.; Guo, Q. X. *J. Phys. Chem. A* **2002**, *106*, 4669.

(13) Cape, J. L.; Bowman, M. K.; Kramer, D. M. *J. Am. Chem. Soc.* **2005**, *127*, 4208.

(14) Markle, T. F.; Rhile, I. J.; DiPasquale, A. G.; Mayer, J. M. *Proc. Natl. Acad. Sci. U.S.A.* **2008**, *105*, 8185.

(15) Costentin, C.; Robert, M.; Savéant, J. M. *Phys. Chem. Chem. Phys.* **2010**, *12*, 11179.

(16) Costentin, C.; Robert, M.; Savéant, J. M.; Tard, C. *Phys. Chem. Chem. Phys.* **2011**, *13*, 5353.

(17) Mayer, J. M. *Annu. Rev. Phys. Chem.* **2004**, *55*, 363.

(18) Huynh, M. H. V.; Meyer, T. J. *Chem. Rev.* **2007**, *107*, 5004.

(19) Benisvy, L.; Bittl, R.; Bothe, E.; Garner, C. D.; McMaster, J.; Ross, S.; Teutloff, C.; Neese, F. *Angew. Chem., Int. Ed.* **2005**, *44*, 5314.

(20) Sjödin, M.; Styring, S.; Åkermark, B.; Sun, L. C.; Hammarström, L. *J. Am. Chem. Soc.* **2000**, *122*, 3932.

(21) Zhang, M.-T.; Irebo, T.; Johansson, O.; Hammarström, L. *J. Am. Chem. Soc.* **2011**, *133*, 13224.

(22) Roberts, J. A.; Kirby, J. P.; Nocera, D. G. *J. Am. Chem. Soc.* **1995**, *117*, 8051.

(23) Deng, Y. Q.; Roberts, J. A.; Peng, S. M.; Chang, C. K.; Nocera, D. G. *Angew. Chem., Int. Ed.* **1997**, *36*, 2124.

(24) Roberts, J. A.; Kirby, J. P.; Wall, S. T.; Nocera, D. G. *Inorg. Chim. Acta* **1997**, *263*, 395.

(25) Concepcion, J. J.; Brennaman, M. K.; Deyton, J. R.; Lebedeva, N. V.; Forbes, M. D. E.; Papanikolas, J. M.; Meyer, T. J. *J. Am. Chem. Soc.* **2007**, *129*, 6968.

(26) Irebo, T.; Reece, S. Y.; Sjödin, M.; Nocera, D. G.; Hammarström, L. *J. Am. Chem. Soc.* **2007**, *129*, 15462.

(27) Freys, J. C.; Bernardinelli, G.; Wenger, O. S. *Chem. Commun.* **2008**, 4267.

(28) Gagliardi, C. J.; Westlake, B. C.; Kent, C. A.; Paul, J. J.; Papanikolas, J. M.; Meyer, T. J. *Coord. Chem. Rev.* **2010**, *254*, 2459.

(29) Lebedeva, N. V.; Schmidt, R. D.; Concepcion, J. J.; Brennaman, M. K.; Stanton, I. N.; Therien, M. J.; Meyer, T. J.; Forbes, M. D. E. *J. Phys. Chem. A* **2011**, *115*, 3346.

(30) Wenger, O. S. *Chem.—Eur. J.* **2011**, *17*, 11692.

(31) Westlake, B. C.; Brennaman, M. K.; Concepcion, J. J.; Paul, J. J.; Bettis, S. E.; Hampton, S. D.; Miller, S. A.; Lebedeva, N. V.; Forbes, M. D. E.; Moran, A. M.; Meyer, T. J.; Papanikolas, J. M. *Proc. Natl. Acad. Sci. U.S.A.* **2011**, *108*, 8554.

(32) Stewart, D. J.; Brennaman, M. K.; Bettis, S. E.; Wang, L.; Binstead, R. A.; Papanikolas, J. M.; Meyer, T. J. *J. Phys. Chem. Lett.* **2011**, *2*, 1844.

(33) Bronner, C.; Wenger, O. S. *J. Phys. Chem. Lett.* **2012**, *3*, 70.

(34) Sacksteder, L.; Zipp, A. P.; Brown, E. A.; Streich, J.; Demas, J. N.; DeGraff, B. A. *Inorg. Chem.* **1990**, *29*, 4335.

(35) Wallace, L.; Rillema, D. P. *Inorg. Chem.* **1993**, *32*, 3836.

(36) Sacksteder, L. A.; Lee, M.; Demas, J. N.; DeGraff, B. A. *J. Am. Chem. Soc.* **1993**, *115*, 8230.

(37) Connick, W. B.; Di Bilio, A. J.; Hill, M. G.; Winkler, J. R.; Gray, H. B. *Inorg. Chim. Acta* **1995**, *240*, 169.

(38) Chen, P. Y.; Westmoreland, T. D.; Danielson, E.; Schanze, K. S.; Anthon, D.; Neveux, P. E.; Meyer, T. J. *Inorg. Chem.* **1987**, *26*, 1116.

(39) Schanze, K. S.; MacQueen, D. B.; Perkins, T. A.; Cabana, L. A. *Coord. Chem. Rev.* **1993**, *122*, 63.

(40) Katz, N. E.; Mecklenburg, S. L.; Meyer, T. J. *Inorg. Chem.* **1995**, *34*, 1282.

(41) Crane, B. R.; Di Bilio, A. J.; Winkler, J. R.; Gray, H. B. *J. Am. Chem. Soc.* **2001**, *123*, 11623.

(42) Gabrielsson, A.; Hartl, F.; Zhang, H.; Smith, J. R. L.; Towrie, M.; Vlcek, A.; Perutz, R. N. *J. Am. Chem. Soc.* **2006**, *128*, 4253.

(43) Hanss, D.; Walther, M. E.; Wenger, O. S. *Chem. Commun.* **2010**, *46*, 7034.

(44) Blanco-Rodríguez, A. M.; Towrie, M.; Sykora, J.; Záliš, S.; Vlček, A. *Inorg. Chem.* **2011**, *50*, 6122.

(45) Kirgan, R.; Simpson, M.; Moore, C.; Day, J.; Bui, L.; Tanner, C.; Rillema, D. P. *Inorg. Chem.* **2007**, *46*, 6464.

(46) Oshin, K.; Landis, A. M.; Smucker, B. W.; Eichhorn, D. M.; Rillema, D. P. *Acta Crystallogr., Sect. E* **2004**, *60*, m1126.

(47) Perkins, T. A.; Hauser, B. T.; Eyler, J. R.; Schanze, K. S. *J. Phys. Chem.* **1990**, *94*, 8745.

(48) Duesing, R.; Tapolsky, G.; Meyer, T. J. *J. Am. Chem. Soc.* **1990**, *112*, 5378.

(49) MacQueen, D. B.; Schanze, K. S. *J. Am. Chem. Soc.* **1991**, *113*, 7470.

(50) Lin, R. G.; Fu, Y. G.; Brock, C. P.; Guarr, T. F. *Inorg. Chem.* **1992**, *31*, 4346.

(51) CH_3CN was distilled over P_2O_5 prior to use in spectroscopic experiments. Note that even the highest quality CH_3CN may contain concentrations of H_2O on the order of 0.1 mM or higher.
(52) Stern, O.; Volmer, M. *Phys. Z.* **1919**, *20*, 183.
(53) The linear regression fits were forced to have an intercept of 0.
(54) Caspar, J. V.; Meyer, T. J. *J. Phys. Chem.* **1983**, *87*, 952.
(55) The dip in the luminescence bands at 650 nm is an instrumental artifact.
(56) As noted above, the fits were forced to intercepts of 0.
(57) The signal-to-noise ratio in part b is lower than in part a because the bpz complex has a shorter excited-state lifetime.
(58) Van Wallendael, S.; Rillema, D. P. *Coord. Chem. Rev.* **1991**, *111*, 297.
(59) Westmoreland, T. D.; Schanze, K. S.; Neveux, P. E.; Danielson, E.; Sullivan, B. P.; Chen, P.; Meyer, T. J. *Inorg. Chem.* **1985**, *24*, 2596.
(60) Das, P. K.; Encinas, M. V.; Steenken, S.; Scaiano, J. C. *J. Am. Chem. Soc.* **1981**, *103*, 4162.
(61) Gadosy, T. A.; Shukla, D.; Johnston, L. J. *J. Phys. Chem. A* **1999**, *103*, 8834.
(62) Brede, O.; Orthner, H.; Zubarev, V.; Hermann, R. *J. Phys. Chem.* **1996**, *100*, 7097.
(63) Lind, J.; Shen, X.; Eriksen, T. E.; Merenyi, G. *J. Am. Chem. Soc.* **1990**, *112*, 479.
(64) Mayer, J. M.; Rhile, I. J. *Biochim. Biophys. Acta* **2004**, *1655*, 51.
(65) Berger, S.; Klein, A.; Kaim, W.; Fiedler, J. *Inorg. Chem.* **1998**, *37*, 5664.
(66) Pavlishchuk, V. V.; Addison, A. W. *Inorg. Chim. Acta* **2000**, *298*, 97.
(67) Roundhill, D. M. *Photochemistry and Photophysics of Metal Complexes*; Plenum Press: New York, 1994.
(68) Although potential values with two digits are reported, we note that these numbers represent estimates that are usually accurate to ca. 0.1 V.
(69) Bordwell, F. G.; Cheng, J. P. *J. Am. Chem. Soc.* **1991**, *113*, 1736.
(70) Yamaji, M.; Oshima, J.; Hidaka, M. *Chem. Phys. Lett.* **2009**, *475*, 235.
(71) D'Angelantonio, M.; Mulazzani, Q. G.; Venturi, M.; Ciano, M.; Hoffman, M. Z. *J. Phys. Chem.* **1991**, *95*, 5121.
(72) Rugge, A.; Clark, C. D.; Hoffman, M. Z.; Rillema, D. P. *Inorg. Chim. Acta* **1998**, *279*, 200.
(73) Sun, H.; Hoffman, M. Z. *J. Phys. Chem.* **1993**, *97*, 5014.
(74) Venturi, M.; Mulazzani, Q. G.; Ciano, M.; Hoffman, M. Z. *Inorg. Chem.* **1986**, *25*, 4493.
(75) Anderson, P. A.; Anderson, R. F.; Furue, M.; Junk, P. C.; Keene, F. R.; Patterson, B. T.; Yeomans, B. D. *Inorg. Chem.* **2000**, *39*, 2721.
(76) We assume that methylation and protonation of the pyrazine ligand have similar effects on the reduction potential of this rhenium complex.
(77) Sullivan, B. P.; Meyer, T. J. *J. Chem. Soc., Chem. Commun.* **1984**, 1244.
(78) Walther, M. E.; Grilj, J.; Hanss, D.; Vauthey, E.; Wenger, O. S. *Eur. J. Inorg. Chem.* **2010**, 4843.
(79) Sheldrick, G. M. *SADABS, Version 2.03*; Bruker Analytical X-Ray Systems, Madison, WI, 2000.
(80) Sheldrick, G. M. *SHELXTL, Version 6.12*; Bruker Analytical X-Ray Systems, Madison, WI, 2000.
(81) To be more precise: The reduced *and protonated* forms, i. e., $[Re^{I}(bpy^{-})(CO)_3(pzH)]^{+}$ and $[Re^{I}(bpzH)(CO)_3(py)]^{+}$.
(82) Záliš, S.; Cosani, C.; Cannizzo, A.; Chergui, M.; Hartl, F.; Vlček, A., Jr. *Inorg. Chim. Acta* **2011**, *374*, 578−585.
(83) Walther, M. E.; Wenger, O. S. *Dalton Trans.* **2008**, 6311−6318.
(84) Hanss, D.; Walther, M. E.; Wenger, O. S. *Coord. Chem. Rev.* **2010**, *254*, 2584−2592.

dx.doi.org/10.1021/ic300834c | *Inorg. Chem.* 2012, 51, 8275−8283